Settling and Swimming of Flexible Fluid-Lubricated Foils

M. Argentina, J. Skotheim, and L. Mahadevan

Université de Nice, Institut du Non-Linéaire de Nice, 1361 Routes des Lucioles, 06560 Valbonne, France
Center for Studies in Physics and Biology, The Rockefeller University, New York, New York 10021, USA
Engineering and Applied Sciences, Harvard University, Cambridge, Massachusetts 02138, USA

(Received 6 April 2007; published 30 November 2007)

We study the dynamics of a flexible foil immersed in a fluid and moving close to a rigid wall. Lubrication theory allows us to derive equations of motion for the foil and thus examine the passive settling and the active swimming of a foil. This also allows us to partly answer the long-standing question in cartoon physics—can carpets fly? Our analysis suggests a region in parameter space where one may realize this dream and move the virtual towards reality.

DOI: 10.1103/PhysRevLett.99.224503 PACS numbers: 47.15.gm, 46.40.Jj, 87.19.St

The myth of the flying carpet is ubiquitous in many cultures, conjuring up images of magical and mystical travels. More recently, animators have recycled these images in cartoons, and perhaps the day is not far off when engineers will provide us with a virtual ride on one. From a physical perspective, we might ask if a flying carpet is possible and, if so, under what conditions might it operate. Indeed, the runaway transparency, that bane of seminar speakers which flexes as it flies away, provides an everyday example of this. In the natural world, there are many analogs of a flying carpet—as seen in rays and skates that glide effortlessly through the depths of the ocean, often just above the sea floor. Motivated by this last observation in particular, we consider the limit when a submerged slender active elastic foil is moving close to a wall, shown schematically in Fig. 1. This problem was studied in the context of swimming with a prescribed gait in an infinite Newtonian fluid [1]. More recent studies have focused on prescribing the kinematics of the foil and solving for the optimal motion of the sheet in Newtonian and non-Newtonian fluids [2–4]. In this Letter, we complement these studies by determining the shape and dynamics of a fluid-lubricated flexible foil [5–7] as it slides and settles onto a wall, and further consider the swimming of such a sheet when driven by actively generated internal torques associated with muscles or their artificial analogs.

We focus on cylindrical deformations for simplicity, although we note that skates, rays, and many marine organisms use more complex deformation patterns. Flow in the thin gap is adequately described by lubrication theory [8] so that we may write

$$-\partial_x p + \mu \partial_{zz} u = 0, \qquad \partial_z p = 0, \qquad \partial_x u + \partial_z w = 0, \tag{1}$$

where p is the pressure, μ is the fluid viscosity, $u(x, z)$ is the horizontal velocity, and $w(x, z)$ is the vertical velocity of the fluid. If the sheet moves at a velocity U in the x direction at a distance $h(x)$ from the wall, the corresponding boundary conditions are $u(x, 0) = 0$, $u(x, h) = U$, $w(x, 0) = 0$, $w(x, h) = \partial_t h + U\partial_x h$ so that integrating (1) yields

$$u(x, z) = \frac{\partial_x p}{2\mu}(z^2 - zh) + U\frac{z}{h}, \tag{2}$$

$$\partial_t h + \frac{1}{2}U\partial_x h - \partial_x\left(\frac{\partial_x p}{12\mu}h^3\right) = 0. \tag{3}$$

For a sheet of thickness ξ, density ρ, Young's modulus E (bending stiffness $D \sim E\xi^3$) with an active distributed torque per unit length $f(x, t)$ (due to muscular activity or artificial actuators), immersed in a fluid of density $\rho - \Delta\rho$, horizontal and vertical momentum balance yields

$$\xi\rho\partial_t U = -\left(\mu\frac{U}{h} + \frac{1}{2}h\partial_x p + p\partial_x h\right) + \partial_x T, \tag{4}$$

$$0 = -\Delta\rho g\xi - \partial_{xx}(f + D\partial_{xx}h) + p, \tag{5}$$

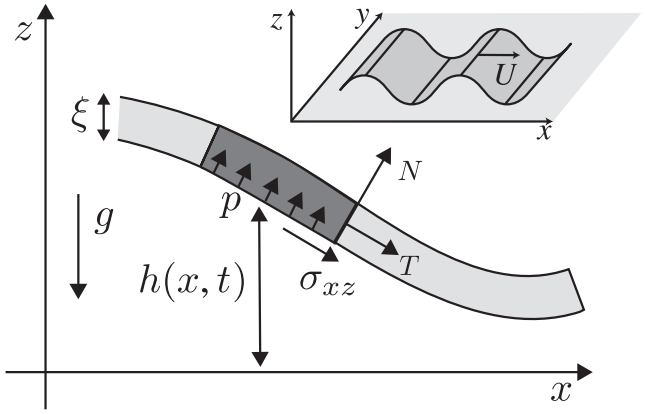

FIG. 1. A schematic of a fluid-lubricated flexible foil flying above the floor ($z = 0$). Here, we also show the various forces and torques on an infinitesimal element of the sheet, with $T(x, t)$ the tension, $M(x, t)$ the torque, $N(x, t)$ the shear force, p the pressure, and σ_{xz} the fluid shear stress. Torque balance implies that $\partial_x M = N$, while normal force balance yields $\partial_x N = p - \Delta\rho g\xi$, which together yield $\partial_{xx} M = p - \Delta\rho g\xi$.

where the second equation was derived in [9] in a slightly different context. Here, the total torque at any cross section, $D\partial_{xx}h + f$, is the sum of the passive elastic torque $M = D\partial_{xx}h$ and the active torque f, while $T(x)$ is the tension, as defined in Fig. 1. We have neglected the inertia of the sheet in the vertical direction, an assumption that is valid when $\rho h_{tt}\xi \ll \Delta\rho g$. Thus for motion with characteristic time scale $\tau \sim L/U$, the sheet must be sufficiently short and close to the wall to satisfy the inequality $L^2 \ll \frac{\Delta\rho}{\rho} gU^2/h$. Furthermore, we have also neglected tension in the vertical momentum balance equation, an assumption that is valid when the sheet is curved only slightly. We now make the system dimensionless by using the definitions $x = Lx'$, $t = \frac{12\mu L^2}{h_0^2\Delta\rho g\xi}t'$, $h = h_0h'$, $p = \Delta\rho\xi g p'$, $U = \frac{\Delta\rho g\xi h_0^2}{6\mu L}U'$ for the scaled variables x', t', h', p', U'. Omitting primes, we write the complete set of equations for a freely moving foil, which are the scaled forms of (3), an integrated form of (4) and (5):

$$\partial_t h + U\partial_x h - \partial_x(h^3\partial_x p) = 0, \tag{6}$$

$$W\partial_t U = -\int_0^1 \left(\frac{U}{h} + 3p\partial_x h\right)dx, \tag{7}$$

$$p = B\partial_{xxxx}h + 1 - \partial_{xx}f. \tag{8}$$

Here $W = \frac{\xi^2 h_0^3\rho\Delta\rho g}{12\mu^2 L^2}$ measures the ratio of horizontal solid inertia to viscous drag, and $B = \frac{hE\xi^2}{12L^4\Delta\rho g}$ measures the ratio of the passive bending elasticity and gravity. Global force and torque balance which result from integrating (8) and its first moment imply that

$$\int_0^1 p\,dx = 1, \qquad \int_0^1 p(x - 1/2)dx = 0. \tag{9}$$

To complete the formulation of the problem, we need some boundary conditions. Since the ends of the sheet are free, they must have no forces or torques, and the pressure must equal the ambient pressure, so that

$$(f - B\partial_{xx}h)|_{0,1} = (\partial_x f - B\partial_{xxx}h)|_{0,1} = p|_{0,1} = 0. \tag{10}$$

We are now ready to address a variety of different problems of increasing complexity. Here we limit ourselves to (i) the settling of a stiff or soft passive sheet, i.e., when $f = 0$, and (ii) the swimming of an active stiff or soft sheet $f \neq 0$.

For a relatively stiff plate falling due to gravity, the shape of the sheet is well approximated by

$$h(x, t) = h_0(t) + (x - 1/2)\gamma(t), \tag{11}$$

where $h_0(t)$ is the average height of the sheet and $\gamma(t) = L\theta/h_0$ is its dimensionless slope. Substituting this ansatz into Eqs. (6) and (9) yields a set of ordinary differential equations which we can easily integrate numerically. In Fig. 2(a), we show that for a tilted plate starting out at rest,

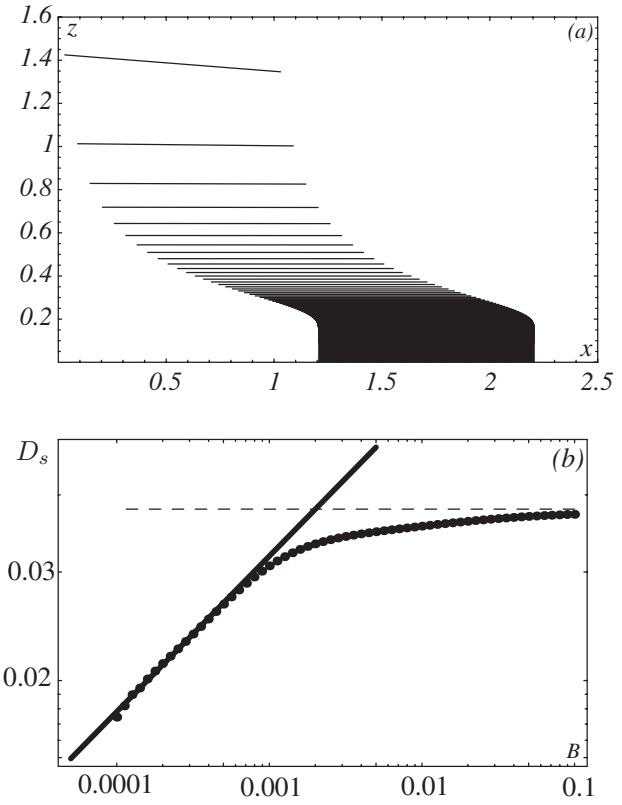

FIG. 2. Falling flexible sheet: (a) Trajectory of a rigid plate obtained by numerical integration of Eqs. (12) for $M = 1$ with initial conditions $h(0) = 2$, $U(0) = 3$, and $\gamma(0) = 0.6$. The plate quickly aligns with the substrate before slowing down as it falls; different lines correspond to snapshots separated by equal time intervals. (b) Scaled sliding distance $D = \mu D_s/\xi\rho h(0)U(0)$ (dotted line) as a function of the nondimensional flexibility B. For a flexible plate $D_s \sim B^{1/4}$ (solid line); when $B \sim O(1)$ the sliding distance approaches the value given by $D_s \sim U(0)\tau \sim \xi\rho h(0)U(0)/\mu$ (see text). Initial conditions are $h(x, 0) = 1$ and $U(0) = 0.1$.

the slope $\gamma(t)$ rapidly decreases to zero as the sheet settles down almost vertically. To understand this, we substitute (11) into (6)–(8) which, to leading order in γ, yields (at leading order)

$$\partial_t h_0 = -12h_0^3 - U\gamma, \qquad W\partial_t U = -\frac{U}{h_0} + \gamma\frac{\partial_t h_0}{4h_0^3},$$
$$\partial_t\gamma = 6\gamma\frac{\partial_t h_0}{h_0}. \tag{12}$$

The solution of (12) for an initially stationary plate, i.e., with $U(0) = 0$ is $h_0 = (\frac{1}{h_0(0)^2} + 24t)^{-1/2}$. Then, it follows that $\gamma \sim h^6 \sim t^{-3} \to 0$; i.e., the plate aligns itself rapidly with the substrate. This is because regions closer to the substrate are subject to higher pressures which force the plate to rotate and align with the substrate. For flexible foils, a similar scenario is observed; the plate becomes nearly horizontal, and the pressure beneath it is almost

constant except in the neighborhood of boundary layers near the two edges where elastic and viscous effects compete.

When the initial velocity of the plate is nonzero, it slides for a while as it settles under its own weight before coming to rest. The characteristic sliding distance that the plate can travel is obtained by balancing the change in the initial momentum with the viscous drag, embodied in (4) and (7), and yields the travel time $\tau \sim \frac{\xi \rho h(0)}{\mu}$ so that the sliding distance for a rigid plate $D_s \sim U(0)\tau \sim \xi \rho h(0) U(0)/\mu$. A more careful computation using (12) yields $\mu D_s/\rho h(0)\xi U(0) \approx 0.379$ for $h(x,0) = W = 1$. When the foil is not rigid, we use a simple finite difference scheme to determine the dependence of the sliding distance D_s on the scaled foil flexibility B by solving (6)–(8) numerically. The results shown in Fig. 2 indicate that stiffer plates travel farther than softer plates. This is because flexibility causes parts of the foil to bend up close to the wall, which slows it down enormously. In this regime, the size of the boundary layer l_B over which bending effects are important are given by (8), which yields $Bh(0)/l_B^4 \sim 1$ so that $l_B \sim (Bh(0))^{1/4}$. This suggests the following scaling for the sliding distance $D_s \sim \frac{\xi \rho h(0) U(0)}{\mu} l_B$, consistent with our numerical results, shown in Fig. 2.

Having understood the case of a passive sheet falling and sliding under its own weight, we now address the dynamics of an active flexible sheet, i.e., the autonomous swimming sheet and its natural counterparts. We denote the time-averaged power delivered by the active torque as $\mathcal{P}$, while the averaged viscous power dissipated in the fluid as $\mathcal{S}$, where

$$\mathcal{P} = \frac{1}{T}\int_0^T \int_0^L (\partial_{xx} f)(\partial_t h) dx dt,$$

$$2\mathcal{S} = \frac{\mu}{T}\int_0^T \int_0^L \int_0^h (\partial_z u)^2 dz dx dt = \mathcal{S}_s + \mathcal{S}_u,$$

where $\mathcal{S}_s = \int_0^L (U^2/h) dx$ and $\mathcal{S}_u = \int_0^1 \frac{(\partial_x p)^2}{12\mu} h^3 dx$ are, respectively, the steady power required to drag a plate at a distance h from a wall (in the absence of gravity), and the unsteady power required to generate lift or thrust via unsteady motions. Since the functional space spanned by the active torque $f(x,t)$ is infinite, we study the problem using an inverse method by imposing the shape of the sheet and using this to deduce the form of f. We assume that the shape of the sheet is a generalization of (11)

$$h(t,x) = h_0(t) + \gamma(t)x + A\sin(\omega t - qx), \qquad (13)$$

where the third term represents the actively generated oscillatory motion of amplitude A, frequency ω, and wave number q.

Equations (6)–(8) together with the boundary conditions (10) constitute a fourth order system for the functions $f(x,t)$, $p(x,t)$ and the parameters $h_0(t)$, $\gamma(t)$. For a given ansatz (13) we use a Newton-Raphson method to determine h_0 and γ by solving (6) and (8) subject to the boundary conditions (10), and to determine U by using (7). In Fig. 3, we show the results of our numerical experiments for a typical parameter set corresponding to a perfectly flexible sheet with $B = 0$; after a short transient, the sheet reaches a periodic steady state and moves with an average velocity $\mathcal{U}$ at an average height h_0 with an average tilt γ.

In Fig. 4(a) we show the average velocity and power [9] as a function of the wave amplitude A; the velocity increases monotonically as A is increased, but the power shows a maximum for some value of the amplitude. Large velocities require large amplitudes of oscillation. However, since the dissipation is dominated by regions of small h, we see a crossover in the power required which actually decreases beyond a critical amplitude (for a given frequency), since the sheet is farther away on average. In Fig. 4(b), we show that as the forcing frequency ω is changed, the velocity and the driving power increase monotonically; one might expect a nonmonotonic effect due to plate inertia in the vertical direction, but we have neglected this effect here. We also varied the forcing wave number q to study its effect on the velocity and power but find that there is essentially no dependence of the velocity on the wave number, while the power increases monotonically. This is consistent with the fact that the dominant contribution to swimming thrust arises from long wavelength modes that can sweep relatively large volumes of liquid; short wavelength modes do not lead to coherent motion, but will help to support the sheet. The relative independence of the velocity on the stiffness is somewhat surprising, but is consistent with the fact that the dominant force balance in the normal direction is between gravity and hydrodynamic pressure. Finally, we investigate the role of flexibility: we find that the velocity remains almost

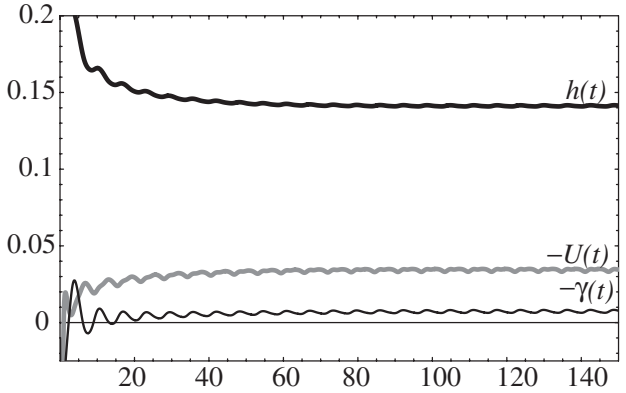

FIG. 3. Motion of an active sheet undergoing periodic sinusoidal deformations with scaled amplitude $A = 0.1$, wave number $q = 25$, and frequency $\omega = 1$ obtained by solving (6)–(10) with the ansatz (13) numerically. We see that the velocity $U(t)$ (thick gray line), height $h(t)$ (thick black line) and tilt $\gamma(t)$ (thin line) shows an initial transient followed by an oscillating steady state.

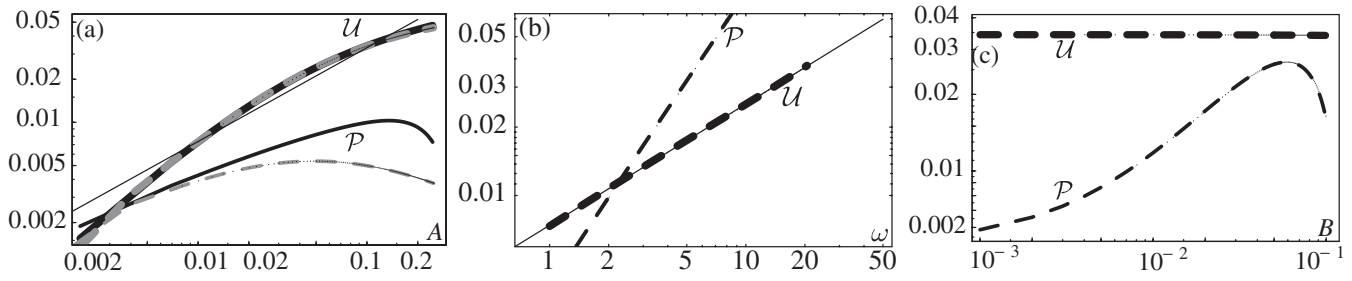

FIG. 4. Average velocity $\mathcal{U}$ and power $\mathcal{P}$ as a function of (a) amplitude of oscillation A, (b) frequency of oscillation ω, and (c) the bending stiffness of the sheet B. The dependence on the wave number q is very weak (data not shown). The parameters used were: for (a) $q = 25$, $\omega = 1$, $B = 0$ (black), and $B = 0.03$ (gray and dashed), the thin solid line is given by $\mathcal{U} \sim A^{2/3}$; for (b) $A = 0.01$ and $q = 25$, $B = 0$, the thin solid line is given by $\mathcal{U} \sim \omega^{2/3}$; for (c) $A = 0.1$, $q = 25$, $\omega = 1$. We also show the power [8] $\mathcal{P}$ required for propulsion, and note $\mathcal{P}$ is a nonmonotonic function of the amplitude A and the bending stiffness B, but increases monotonically with frequency ω. The average speed is consistent with the scaling law $\mathcal{U} \sim (\omega A)^{2/3}$ as derived in the text [see (14)].

constant over a range of B, as shown in Fig. 4(c), but the power required is nonmonotonic as a function of the stiffness; a stiff plate can displace fluid efficiently, while a flexible plate requires little energy to deform it.

To understand these trends, we consider times large compared to those associated with the oscillations of the sheet. Then the fluid pressure must just balance the weight of the sheet, so that $p \sim \Delta\rho g\xi$. Similarly, for a sheet moving at constant velocity, the balance of horizontal forces yields the relation $\mu\mathcal{U}/h_0 \sim p\gamma$. Finally, continuity coupled with horizontal force balance in the fluid yields $\mu\mathcal{U}\gamma \sim ph_0^3/L^2$. Complementing these relations with the kinematic condition $\omega A/q \sim \mathcal{U}\gamma L$, which states that the fluid flow induced by the traveling waves must balance that induced by the steady movement of the sheet, yields the following scaling relations:

$$h_0 \sim \left(\frac{A\omega}{q}\frac{\mu L}{\Delta\rho g\xi}\right)^{1/3}, \quad \mathcal{U} \sim \left(\frac{A\omega}{q}\right)^{2/3}\left(\frac{\Delta\rho g\xi}{\mu L}\right)^{1/3}, \quad (14)$$

and $\gamma \sim h_0/L$. Since we expect only the long wavelength modes to generate movement, we expect that $q \sim 1/L$, so that $\mathcal{U} \sim (A\omega)^{2/3}(\frac{\Delta\rho g\xi L}{\mu})^{1/3}$, qualitatively consistent with the numerical results shown in Figs. 4(a) and 4(b). We see that, to maintain a fast moving sheet, we need a large amplitude and frequency with deformation on scales comparable to the length of the sheet. This is consistent with our developed intuition that the lubrication induced pressure balances the weight of the sheet, while the fluid displaced by the traveling waves propels the sheet.

So, can a transparency or a carpet fly in air? For a 10 cm l ong sheet of thickness 0.1 mm, a forcing frequency $\omega \sim$ 10 Hz, an amplitude of oscillation of order $A \sim 250$ μm, we find that $h_0 \sim 10^{-3}$ m, $U \sim 0.3$ m $\cdot$ s^{-1}, and the active torque $f_{\max} \sim \Delta\rho g\xi/L^2 \sim 10^{-1}$ N $\cdot$ m, all of which are within the realm of possibilities in nature and in technology. Making a heavy carpet fly would, of course, require a much more powerful engine, and our computations and scaling laws suggest it will remain in the magical, mystical, and virtual realm as it has existed for millenia. In air, jet-propelled carpets are quite a different story altogether. In water, where the density contrast between a carpet and water is much less, swimming carpets are easily plausible. Indeed, the common skate or ray shows us nature's own swimming carpet. To move beyond our quantitative analysis of these multiparameter problems now requires a combination of experiments with real biomimetic devices and observations of real organisms.

[1] G. I. Taylor, Proc. R. Soc. A **209**, 447 (1951).
[2] E. Lauga, Phys. Rev. E**75**, 041916 (2007).
[3] N. Balmforth, B. Chan, and A. Hosoi, Phys. Fluids **17**, 113101 (2005).
[4] E. Lauga, Phys. Fluids **19**, 083104 (2007).
[5] E. O. Tuck and M. Bentwich, J. Fluid Mech. **135**, 51 (1983).
[6] W. Gross, L. Matsch, V. Castelli, A. Eshel, J. Vohr, and M. Wildmann, *Fluid Film Lubrication* (Wiley-Interscience, New York, 1980).
[7] R. C. Benson, J. Tribol. **117**, 47 (1995).
[8] G. K. Batchelor, *An Introduction to Fluid Dynamics* (Cambridge University Press, Cambridge, UK, 1967).
[9] A. Hosoi and L. Mahadevan, Phys. Rev. Lett. **93**, 137802 (2004).